

CHAPTER 154

LONGSHORE BAR GENERATION MECHANISMS

Robert G. Dean¹, Rajesh Srinivas¹, and Trimbak M. Parchure²

ABSTRACT

A laboratory study was conducted to investigate mechanisms of bar formation with particular focus on infragravity wave and break point mechanisms. With one exception, all tests commenced with a planar beach composed of fine sand. Infragravity (IG) waves, the result of a biharmonic primary wave spectrum, were generated and documented. For various frequency differences of the components of the primary spectrum and thus the frequencies of the IG wave, the changes in nodal/antinodal positions were compared with the changes in positions of the bar formed during the experiment. It was found that the bar position experienced relatively small movements whereas the nodal/antinodal positions changed substantially as expected with the difference frequency of the primary waves. The approximately constant bar position was interpreted as due to the relatively constant primary wave height characteristics. The effects of the wave spectrum and wave height distribution on bar formation were investigated. The shape of the wave height probability distribution function was found to exert a noticeable control on the degree of bar relief, with those distributions characterized by a substantial concentration near the maximum wave height causing the more prominent bars. This is interpreted in terms of a transport influence function which, if held stationary, would result in a narrow prominent bar. The distributions with a small concentration near the maximum wave height resulted in a less prominent bar. A conceptual model is proposed which incorporates the transport distribution function and which results in bar characteristics which depend on the initial conditions.

¹Coastal and Oceanographic Engineering Department, University of Florida, Gainesville, Florida 32611 USA.

²Hydraulics Laboratory, Waterways Experiment Station, U. S. Army Corps of Engineers, Vicksburg, Mississippi 39801 USA.

INTRODUCTION

Several mechanisms have been proposed for the formation of offshore bars, which can be described as rather low, generally shore-parallel positive features which rise a substantial fraction of the water depth above the sea floor. Bars occur singly or as a series of such features. In many locations of the world, they are correlated with seasons or episodic events of higher wave activity. In other locations, bars are perennial.

Four mechanisms for the formation of bars are reviewed briefly below: (1) Break point, (2) Standing waves formed by reflection from shore back out to sea, (3) Standing edge waves, and (4) Overtake of harmonic waves.

Break Point Mechanism

The break point mechanism ascribes bar formation to the convergence of sediment transport due to either or a combination of sand transport seaward and/or landward towards the final bar position. The primary effect is seaward transport by the breaking process due to the vortex formed as the breaking wave transfers a torque to the water column which causes a local seaward bottom velocity. This seaward flow may be considered as undertow compensating for the landward mass transport. However, this undertow is locally reinforced by the aforementioned breaking induced torque. Bars frequently occur in wave tanks under the action of monochromatic waves. Such bars are referred to as "break point" bars in recognition of their causative mechanism.

Standing Waves Formed by Reflection from Shore Back Out to Sea

A wave propagating toward the shoreline will reflect to some degree from the shoreline forming partial nodes and antinodes. The degree of reflection increases with longer wave periods and steeper beach slopes. The shore parallel nodes and/or antinodes are attractive as an explanation for the bar formation (Sallenger and Howd, 1989). Some proponents of this mechanism suggest that formation can occur under either the nodes or antinodes (Carter et al. 1973). A narrow spectrum will cause the formation of long waves, generally termed as "infragravity" waves with frequency characteristics determined by the spectral width. These long waves reflect efficiently from the beach. It is well-known that bar-like features form in wave tanks under standing wave envelopes.

Edge Waves

The explanation for this mechanism is somewhat similar to that described in the preceding paragraph. The only difference is that edge waves are trapped by reflection thereby maintaining the energy within the nearshore trapping region

whereas for the preceding mechanism, the waves are "leaky" with the reflected energy propagating offshore.

Overtake of Harmonic Waves

The basis for this explanation is the alternate reinforcement and cancellation of waves of periods corresponding to the first harmonic of the dominant fundamental wave (e.g., Buhr Hansen and Svendsen, 1974). Two waves of this frequency are required: one bound to the fundamental by nonlinear mechanisms and a second free wave propagating at its own speed. Since the propagational speeds of these two waves are different, they will interfere, alternatively reinforcing and canceling at positions which, for a uniform water depth, are periodically spaced along the direction of wave propagation. Contrary to most field observations in which the bar spacing decreases with decreasing water depth, the overtake mechanism predicts an increasing bar spacing with decreasing water depth.

EXPERIMENTAL FACILITIES

The experiments described in this study were conducted in the facility shown in Figure 1 which consists of a wave tank with programmable wavemaker. The tank is approximately 37 m long, 2 m wide and 1.3 m deep. A long partition extends from near the wavemaker to the distal end of the tank forming two channels each of 0.9 m width. A beach of initial slope 1:19 was formed of fine sand ($D_{50\%} \approx 0.21$ mm) in one side of the partitioned tank. The wavemaker is driven by hydraulic actuators at two levels, each of which can be controlled independently.

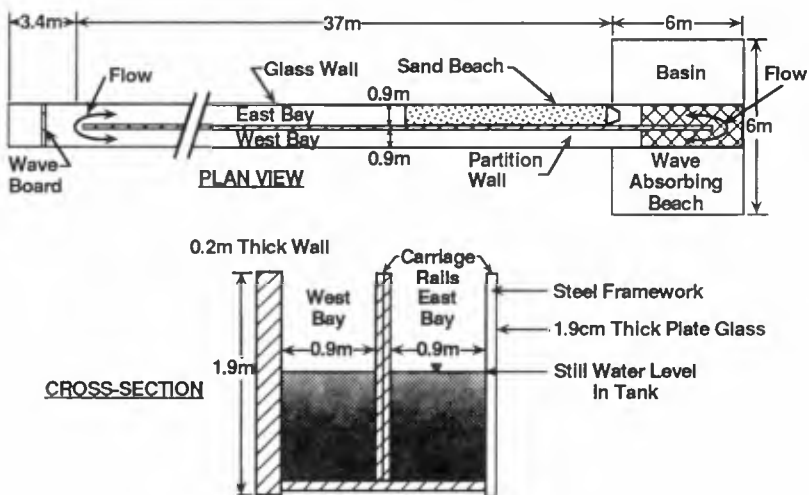


Figure 1. Schematic and Cross-Section of Wave Tank Facility.

INVESTIGATION CHARACTERISTICS AND RESULTS

The experiments have attempted to address the question of bar formation mechanisms as well as the spectral characteristics that will result in the presence of a bar. All tests were conducted for at least 4.5 hours and the profiles appeared to be near equilibrium. Two study components were carried out and are described below.

Correlation of Bar Characteristics And Infragravity Waves

This study component is essentially an extension of that conducted by W. R. Dally (1987) in which the incident wave system was biharmonic, i.e. composed of two discrete components, thus resulting in a pronounced infragravity wave component. Reflection of the infragravity component from the wavemaker, an artificiality due to the wave tank, increased its amplitude; the locations of the nodes and antinodes were fixed by the long wave period and the beach profile. The infragravity wave characteristics were measured by a manometer and stilling well apparatus that damped the primary waves. An example of the primary and long wave systems and their associated spectra is presented in Figure 2. The associated wave height probability distribution function and initial and final beach profiles are presented in Figure 3. The method of relating the bar and nodal/antinodal positions to test this hypothesis differed from that of Dally. A total of four experiments of this type was carried out: the analysis and results will be described later.

In addition to documenting the long wave envelope structures generated in the laboratory, they were calculated considering the long wave to be free and represented by the following equation

$$\sigma^2 \eta + g \frac{\partial}{\partial x} \left(h \frac{\partial \eta}{\partial x} \right) = 0$$

which was formulated and solved in finite difference form and found to compare favorably with the analytical solution for a planar beach

$$\eta = J_0 \left(2\sqrt{\kappa x} \right)$$

where

$$\kappa = \frac{\sigma^2}{g m}$$

and J_0 is the zeroth order Bessel function of the first kind, σ is the long wave angular frequency, g is gravity and m is the profile slope. The agreement was found to be good. Figure 4 presents an example of calculated and measured long wave envelopes for Case 3.

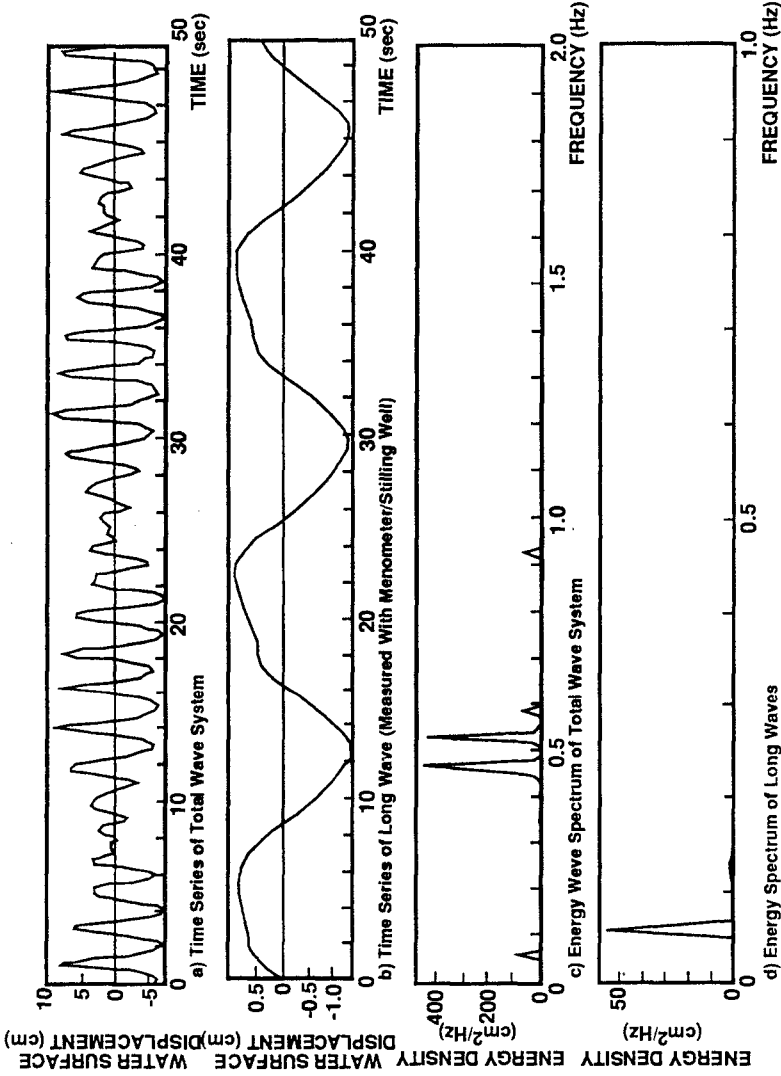
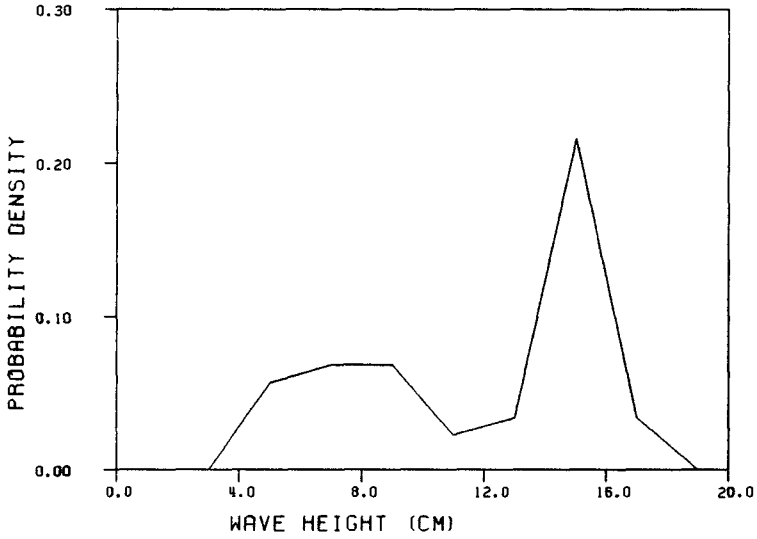
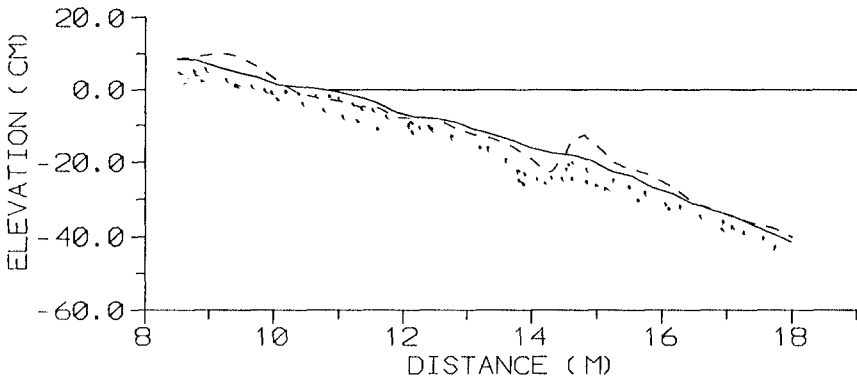


Figure 2. Case 1. Biharmonic Waves. Primary Wave Frequencies = 0.47 and 0.53 Hz.
 Maximum Primary Wave Height \approx 16 cm.



a) Wave Height Probability Distribution for Case 1.



b) Initial (Solid) and Final (Dashed) Profiles for Case 1.

Figure 3. Wave Height Probability Distribution and Initial and Final Profiles for Case 1.

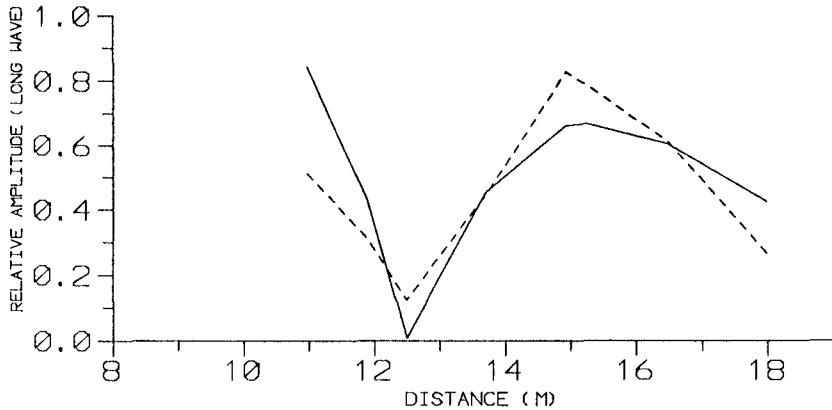


Figure 4. Comparison of Measured (Dashed) and Computed (Solid) Long Wave Envelopes for Case 3.

Table 1 summarizes the positions of the bar and nearest measured IG wave node and antinode. Plotted in Figure 5 is the relationship between the measured changes in bar and measured IG wave nodal/antinodal positions. The changes are relative to the next lower difference frequency (Table 1). If the bar were formed by the infragravity wave system, it is expected that a change in the IG nodal/antinodal position from one frequency to another would correspond to exactly the same change in bar position. Stated differently, the points in Figure 5 should fall along a straight line inclined at 45° , whereas although the positions of the nodes and antinodes changed as expected with IG frequency, the bar location experienced little change. Based on these results, the hypothesis that the bar is caused by the position of envelope of the IG wave is rejected. The nearly unchanging position of the bar position with nearly constant wave height supports the break point hypothesis of bar formation.

Effect of Wave Spectra and Wave Height Probability Characteristics on Bar Formation

A series of experiments was conducted to attempt to identify the effects of different incident wave spectral characteristics on bar formation. Table 2 summarizes the characteristics of these tests. Both continuous and discrete spectral shapes were tested. Figures 2 and 3 have presented an example for Case 1 showing primary and long wave records, the associated probability distributions and resulting profiles. Similar results for Case 5 are presented in Figures 6 and 7. Figure 8 documents the wave height probability distribution and initial and final profiles for Case 7 and the profiles for Case 8.

Table 1

Characteristics of Experiments with Biharmonic Primary Waves

Case	Primary Frequencies (Hz)	Difference Frequencies (Hz)	Nodal Position (m)	Antinodal Position (m)	Bar Position (m)
1	0.47, 0.53	0.06	14.3	15.3	14.8
2	0.46, 0.54	0.08	13.5	15.0	14.9
3	0.45, 0.55	0.10	12.5	15.0	14.8
4	0.44, 0.56	0.12	11.6	13.1	14.5

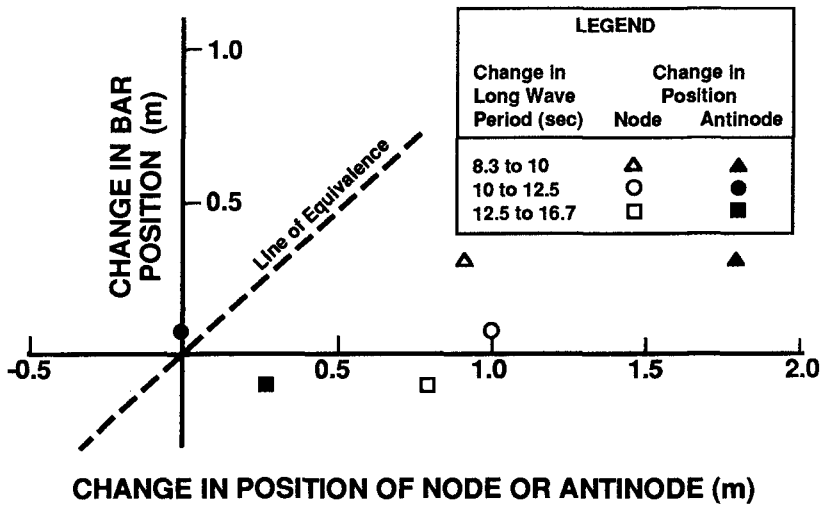


Figure 5. Change in Bar Position vs. Change in Positions of Nodes and Antinodes. Biharmonic Waves.

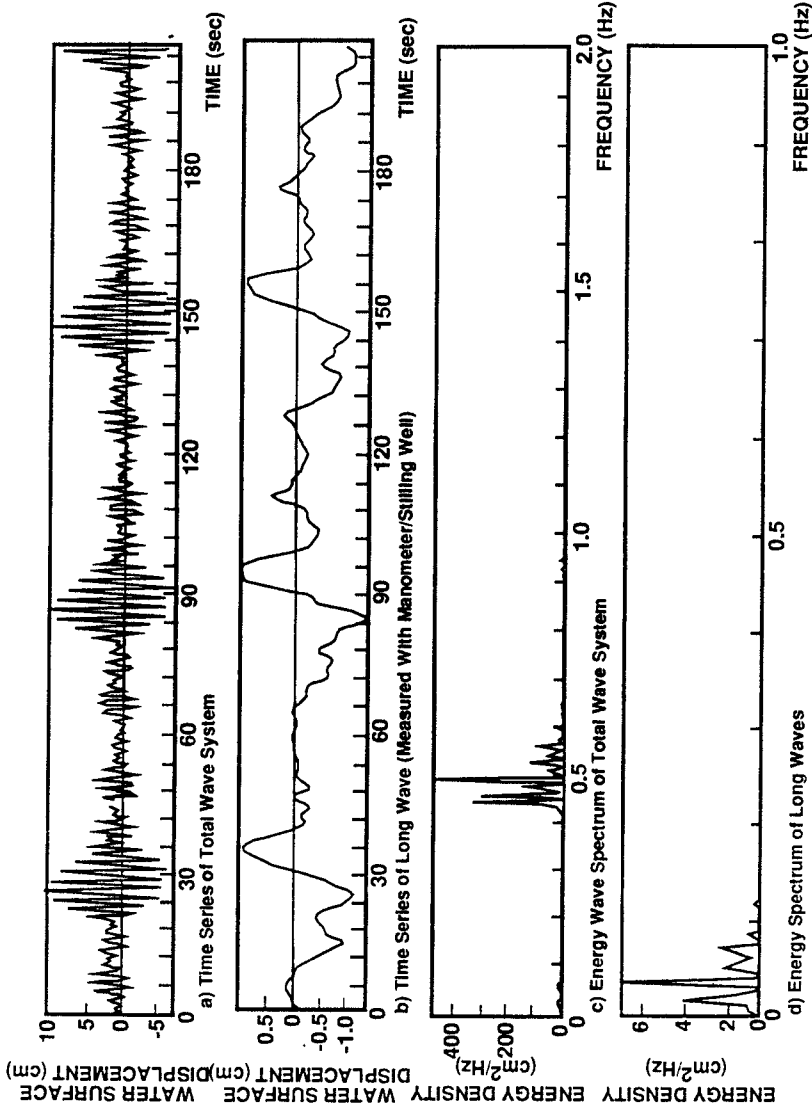
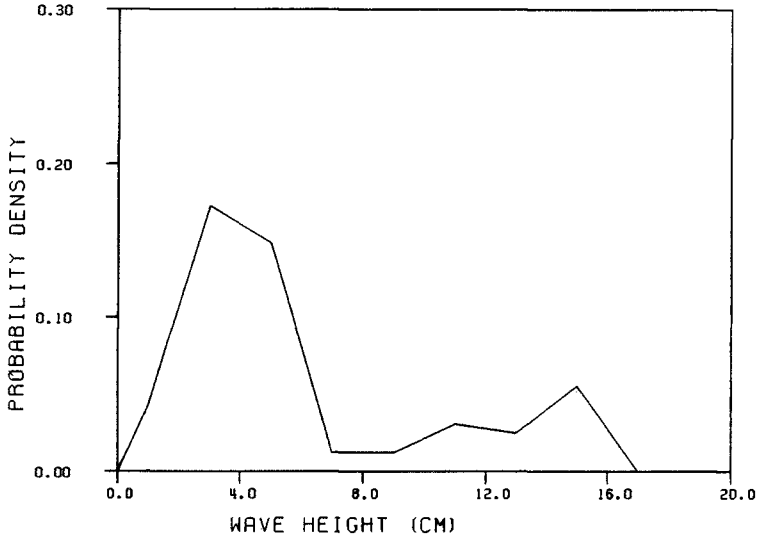
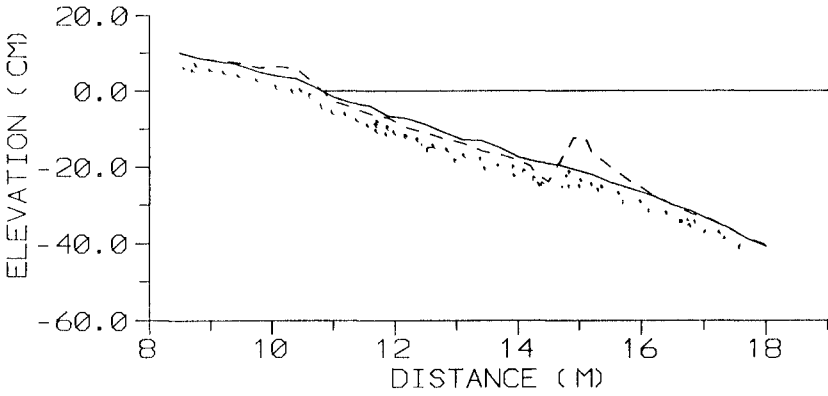


Figure 6. Case 5. Multifrequency Waves. Maximum Primary Wave Height \approx 16 cm.

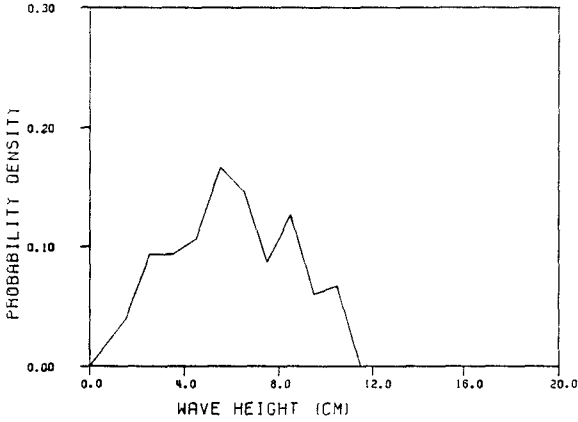


a) Wave Height Probability Density Function

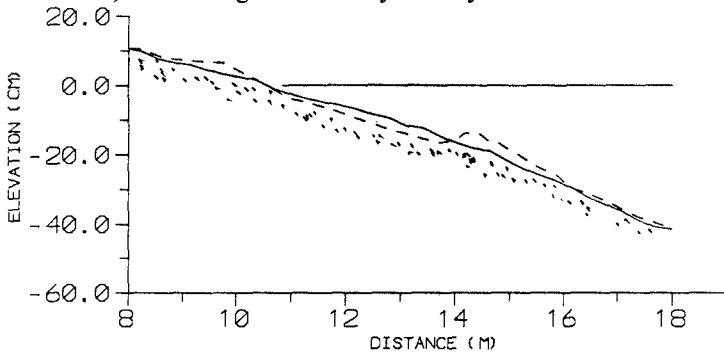


b) Initial (Solid) and Final (Dashed) Profiles

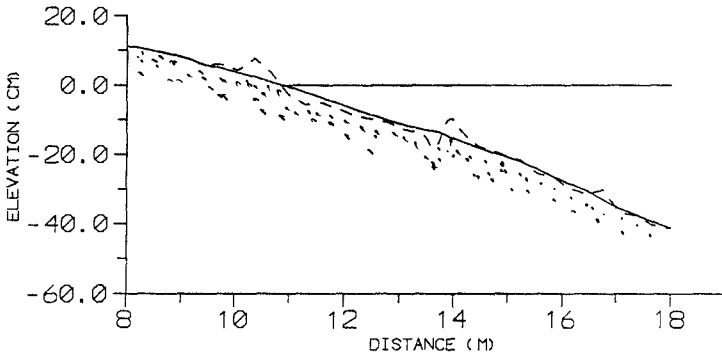
Figure 7. Case 5. Wave Height Probability Density Function and Initial and Final Profiles.



a) Wave Height Probability Density Function. Case 7.



b) Initial (Solid) and Final (Dashed) Profiles. Case 7.



c) Initial (Solid) and Final (Dashed) Profiles. Case 8.

Figure 8. Wave Height Characteristics (Case 7) and Profiles (Cases 7 and 8).

Table 2
Test Characteristics for Various Spectral Characteristics

Case	Initial Profile	Spectral Character.	Mean Freq. (Hz)	Final Bar Position (m)	Maximum Wave Height (m)
5	Planar	Multifreq.	0.5	15.0	0.16
6	Barred	Multifreq.	0.5	15.0	0.16
7	Planar	Continuous	0.5	14.3	0.11
8	Planar	Monochrom.	0.5	13.9	0.11

The effects of the wave height probability density (WHPD) function are evident by comparing Figures 3, 7 and 8. The WHPD functions for Cases 1 and 5 have either primary or secondary peaks near the maximum wave height, whereas for Case 7, the most probable wave heights occur at a height of approximately one-half the maximum height. For Case 8 (monochromatic), the peak is at the maximum wave height. The final profiles for all cases with primary or secondary peaks near the maximum wave heights have pronounced bars whereas the final profile for the WHPD function with no peak near the maximum wave height is relatively subtle and diffuse (Figures 8a and 8b). Also, it was noticed during the experiments that the rate of evolution towards a fully developed bar was more rapid for those WHPD functions with a primary peak near the maximum wave height.

SUGGESTED MECHANISM FOR BAR FORMATION

Based on the results of this and previous studies, the following model is proposed for bar formation. The break point mechanism is responsible for the type of bars investigated here in the laboratory. Moreover, they also apply to bars that we have investigated in the field (Dolan and Dean 1985).

In order for bars to form, the fall velocity parameter $H_0/(wT)$ (H_0 = deep-water wave height, w = sediment fall velocity and T = wave period) must be greater than approximately 3 (Kriebel et al. 1986). Multiple bars require a sufficiently mild slope such that wave reformation and multiple breaking occurs. For conditions that are marginally favorable for bar formation, the probability distribution of breaking wave heights can result in non-formation if the WHPD function does not have a peak near the maximum wave height. Bars tend to be self maintaining by trapping waves to break on the bars. Conditions that are marginally favorable for bar formation can form a prominent bar if a bar feature is initially present.

The mechanism for bar formation can be considered in terms of a transport influence function, $f(x')$ where x' is the local coordinate fixed to the time-varying breaking point and the function $f(x')$ is scaled according to the breaking wave height or wave energy dissipation per unit water volume. Seaward of the breaking point the transport is landward, and landward of the breaking point the transport is directed seaward. When intense breaking wave conditions extend across a wide breaking zone, the net bar generating transport mechanisms are diminished relative to a stable breaking wave position. To reach equilibrium, there must be a negative feedback on the influence function. The failure to date to adequately define this feedback mechanism appears to be one of the major impediments in our attempts to quantify the full mechanisms for bar formation and equilibration.

SUMMARY AND CONCLUSIONS

A series of wave tank experiments has been conducted to investigate mechanisms of bar formation. Conditions encompassed monochromatic waves and a variety of wave spectra, including cases specifically planned to generate and document the characteristics of the infragravity waves known to accompany a narrow spectrum of primary waves. The conclusions reached from this investigation are presented in the following paragraphs.

The tests conducted with two primary waves which produced a long standing wave were analyzed and the changes in bar position and changes in long wave nodal/antinodal positions compared. It was found that while the long wave nodal/antinodal positions changed as expected with the long wave period, the bar position experienced relatively small displacements. It is concluded that the bar position is governed by the breaking position rather than the long wave envelope structure.

Tests were conducted with a range of spectral shapes and a corresponding range of wave height probability density functions. It was found that for the tests conducted with a density function characterized by a primary or secondary peak near the maximum wave height, intense breaking occurred over a smaller range of positions and the bar was more accentuated and concentrated in position. For conditions with a maximum density near the mid-range of wave heights, breaking occurred over a correspondingly broader range of positions and the bar was somewhat more subdued and less concentrated. These results are interpreted as the result of the dynamic equilibrium in which, as the bar breaks at a particular location, it induces bar formation transport mechanisms; however, due to the aforementioned variation in breaking wave position, the breakpoint transport pattern is not positionally stable for a sufficient duration to cause the bar to form to the degree that would occur under a constant breaking position. On the basis of these findings, a conceptual model for bar formation is proposed, which has as a significant element, a transport influence function with characteristics near the breakpoint that tend to result in bar formation. Depending on the wave height

distribution function and the initial beach profile characteristics, the break point ranges across the active profile and thus results in a dynamic equilibrium.

It is hoped that the results presented herein will stimulate further research on bar formation which will either support the mechanisms presented here or will lead to a more thorough understanding and robust models of bar formation and maintenance.

ACKNOWLEDGEMENT

The support of the Florida Department of Natural Resources for the work described in this paper is gratefully acknowledged.

REFERENCES

- Buhr Hansen, J. and I.A. Svendsen (1974) "Laboratory Generation of Waves of Constant Form", Proceedings of the 14th Conference on Coastal Engineering, American Society of Civil Engineers, pp. 321-339.
- Carter, T.G., P.L.F. Liu and C.C. Mei (1973) "Mass Transport by Waves and Offshore Sand Bedforms", Journal of Waterways, Harbors and Coastal Engineering Division, American Society of Civil Engineers, Vol. 99, pp. 165-184.
- Dally, W.R. (1987) "Longshore Bar Formation- Surf Beat or Undertow?", Proceedings of the ASCE Specialty Conference on Coastal Sediments '87, pp.71-86.
- Dolan, T.J. and R.G. Dean (1985) "Multiple Longshore Sand Bars in the Upper Chesapeake Bay", Journal of Estuarine, Coastal and Shelf Science, Vol. 21, pp. 727-743.
- Kriebel, D.L., W.R. Dally and R. G. Dean (1986) "Undistorted Froude Model for Surf Zone Sediment Transport", Proceedings of the 20th Coastal Engineering Conference, American Society of Civil Engineers, Vol. 2, pp. 1393-1406.
- Sallenger, A.H. and P.A. Howd (1989) "Nearshore Bars and the Break-Point Hypothesis", Journal of Coastal Engineering, Vol.12, pp. 301-313.